HHS Public Access

Author manuscript

Ann Thorac Surg. Author manuscript; available in PMC 2016 March 01.

Published in final edited form as:

Ann Thorac Surg. 2015 March ; 99(3): 911–917. doi:10.1016/j.athoracsur.2014.10.043.

Relationship of Single Ventricle Filling and Preload to Total Cavopulmonary Connection Hemodynamics

Christopher M. Haggerty, PhD[1], **Kevin K. Whitehead, MD, PhD**[2], **James Bethel, PhD**[3], **Mark A. Fogel, MD**[2], and **Ajit P. Yoganathan, PhD**[1]

[1]Wallace H. Coulter Department of Biomedical Engineering, Georgia Institute of Technology & Emory University, Atlanta, GA, USA

[2]Division of Pediatric Cardiology, The Children's Hospital of Philadelphia, Philadelphia, PA, USA

[3]Westat, Inc., Rockville, MD, USA

Abstract

Background—Single ventricle lesions are associated with gradual attrition following surgical palliation with the total cavopulmonary connection (TCPC). Ventricular dysfunction is frequently noted, particularly impaired diastolic performance. This study seeks to relate TCPC hemodynamic energy losses to single ventricle volumes and filling characteristics.

Methods—Cardiac magnetic resonance (CMR) data were retrospectively analyzed for 30 single ventricle patients at an average age of 12.7 ± 4.8 years. Cine ventricular short axis scans were semi-automatically segmented for all cardiac phases. Ventricular volumes, ejection fraction, peak filling rate, peak ejection rate, and time to peak filling were calculated. Corresponding patient-specific TCPC geometry was acquired from a stack of transverse CMR images; relevant flow rates were segmented from through-plane phase contrast CMR data at TCPC inlets and outlets. TCPC indexed power loss was calculated from computational fluid dynamics simulations using a validated custom solver. Time-averaged flow conditions and rigid vessel walls were assumed in all cases. Pearson correlations were used to detect relationships between variables, with $p<0.05$ considered significant.

Results—Ventricular end diastolic ($R = -0.48$) and stroke volumes ($R = -0.37$) had significant negative correlations with the natural logarithm of a flow-independent measure of power loss. This power loss measure also had a significant positive relationship to time to peak filling rate (normalized to cycle time; $R=0.67$).

Address for Correspondence: Ajit P. Yoganathan, PhD, The Wallace H. Coulter Distinguished Faculty Chair in Biomedical Engineering & Regent's Professor, Associate Chair for Translational Research, Wallace H. Coulter Department of Biomedical Engineering Georgia Institute of Technology & Emory University, 387 Technology Circle, Suite 232, Atlanta, GA 30313-2412, ajit.yoganathan@bme.gatech.edu; Phone: 404-894-2849; Fax: 404-385-1268.

Conclusions—Flow-independent TCPC power loss is inversely related with ventricular end diastolic and stroke volumes. Elevated power losses may contribute to impaired diastolic filling and limited preload reserve in single ventricle patients.

Keywords

CHD, Fontan; Bioengineering (incl modeling); cardiac function, physiology

INTRODUCTION

In the present era, operative mortality of the Fontan procedure for single ventricle heart defects is low but shortened life expectancy is a significant problem(1). The contributions of ventricular dysfunction to these outcomes is well understood. Decreased systolic performance in the forms of reduced cardiac index(2) and ejection fraction(3) have been widely reported. More recently, appreciation for the incidence and importance of impaired diastolic performance has also grown. Anderson *et al.* reported abnormal diastolic function in 72% of a 500 patient cohort(4), while Cheung *et al*. found reduced ventricular relaxation times via echocardiography that are suggestive of reduced compliance(5).

While fundamental deficiencies in myocardial structure may be central to this impaired diastolic performance, the effect of altered vascular function may also play a role. Limited preload reserve and reduced ventricular filling with increasing heart rate(6) are prime examples of such interactions. In this setting, the potential contributions of the total cavopulmonary connection (TCPC), the surgical palliation for single ventricle defects, are not well understood. The hemodynamics of this connection have been the focus of a large volume of research (7-11) with the general hypothesis that inefficient and sub-optimal flow patterns would have negative implications for broader cardiovascular health and function. While insightful, these studies have mostly been performed in isolation (i.e., focused only on the TCPC) and not inclusive of broader physiologic end points against which TCPC hemodynamics could be compared to further advance understanding. For example, no study to date has evaluated the associations between TCPC hemodynamics and single ventricle function based on patient data.

In this study, we analyzed concurrent data for ventricular function and patient-specific TCPC power loss, one important component of the hemodynamic profile, using image-based computational fluid dynamics (CFD) simulations(9, 12) for a group of single ventricle patients after the Fontan procedure. We hypothesize that elevated TCPC power losses are associated with impaired ventricular filling and volumes.

PATIENTS AND METHODS

Patient Selection

Forty-four consecutive single ventricle patients from the NIH-supported Georgia Tech-Children’s Hospital of Philadelphia Fontan Cardiac Magnetic Resonance database were selected for analysis on the basis of the retrospective availability of (1) a ventricular short axis cine image stack spanning the entire ventricular volume, (2) a transverse stack of

steady-state free precession images through the thorax, and (3) cross-sectional through plane phase contrast magnetic resonance acquisitions at all TCPC inlets and outlets. The data from (1) were used to quantify ventricular function, (2) was used to create a patient-specific TCPC model and (3) are the needed inputs for computational fluid dynamics simulations to assess local TCPC hemodynamics. All images were acquired on a 1.5-T Siemens Magnetom Avanto (Siemens Medical Systems). The imaging details are provided in Table 1. The Institutional Review Boards at the Children's Hospital of Philadelphia and Georgia Tech approved the study, and informed consent was obtained for each patient.

Ventricular Segmentation

Semi-automatic segmentation of the ventricular cavity was performed at Georgia Tech using an in-house algorithm implemented in Matlab (The Mathworks, Inc., Natick, MA) and based on active contours. An endocardial contour was initialized on the first phase (end diastole) for a given slice and propagated through the rest of the cine set. Manual corrections were made as necessary to ensure a visually appropriate segmentation. Papillary muscles were included in the blood pool. Once the stack was entirely segmented, the ventricular volume of each cardiac phase was calculated by summing the products of the cross-sectional areas and slice thicknesses. These measurements were used to derive ventricular volumes, ejection fraction, and cardiac output. Additionally, a smooth ventricular volume vs. time curve was generated using a Fourier curve fitting analysis with the use of 3 harmonics(13); the first derivative of this curve was then computed to derive the maximum time rates of volume change (i.e., peak ejection rate and peak filling rate(6)), and time to peak filling rate (from end systole). The peak filling and ejection rates are presented normalized by end diastolic volume [s^{-1}]. Time to peak filling rate was normalized to cardiac cycle time and reported as a 'time ratio'(14).

To verify the precision of the segmented volumes, inter- and intra-observer variability was assessed on a select number of patient data sets. For inter-observer variability, another expert user separately segmented the end diastolic and end systolic phases for eight patients. For intra-observer variability, segmentations for five patients were repeated by the same user 7-8 months following the initial analysis.

TCPC Hemodynamic Assessment

Computational fluid dynamics models are the current standard for quantifying TCPC flow associated energetics(9, 14, 15) because of their excellent spatial resolution and their ability to robustly handle patient-specific connections. In this study, hemodynamics through the TCPC were assessed using a validated(12, 16) in-house computational fluid solver based on the hybrid Cartesian immersed boundary method(17). The transverse abdominal image stack and through-plane phase contrast magnetic resonance imaging data were used to provide the anatomic(18) and patient-specific flow(19) boundary conditions, respectively, needed to perform the computational simulations (see Figure 1). Since the primary CFD end point was a representative, time-averaged measure of power loss, the patient-specific simulations assumed time-averaged boundary conditions based on the phase contrast CMR data measured for each vessel and for each patient. Recent studies have demonstrated that this approach yields power loss estimates with acceptable limits of agreement compared to

simulations with time-varying boundary conditions(20). The inlets were artificially extended by 1 cm and a flat velocity profile was imposed at the extended inlets to ensure partially developed flow (as would be expected physiologically) at the entrance to the domain of interest. The outlets were similarly extended by 5 cm to prevent flow reversal in the computations, and flow boundary conditions were imposed based on the ratio of measured vessel flow to total pulmonary arterial flow. The governing fluid mechanics equations were solved in their complete unsteady formulation assuming blood to be a Newtonian fluid of constant viscosity (3.71 $kg \cdot m^{-1} \cdot s^{-1}$) and density (1060 $kg \cdot m^{-3}$). Vessel walls were assumed to be rigid, which is consistent with the assumption of time-averaged flow.

The primary end point was the time-averaged power loss (PL) through the connection, calculated as:

$$PL = \sum_{inlets} \int_A \left(p + \frac{1}{2}\rho v^2 \right) v \cdot dA - \sum_{outlets} \int_A \left(p + \frac{1}{2}\rho v^2 \right) v \cdot dA$$

where p is the static pressure, ρ is density, A is vessel area, and v the velocity. Because power loss is highly dependent on the flow rate, a flow-independent power loss index was computed:

$$\frac{PL}{\rho \cdot Q^3 \cdot BSA^{-2}},$$

where Q is systemic venous flow rate and BSA is the body surface area. Just as the cardiac index is a body size-independent measure of ventricular output, this index, which was previously derived using an established engineering method of dimensional analysis(21), is a flow-independent index of TCPC power loss (iPL).

Statistical Analysis

Statistical analyses were performed using SPSS (IBM, Inc., Armonk, NY). Pearson's R was used for correlations between functional variables; partial correlation was used, as needed, to correct for the confounding effects of other independent variables. P-values less than 0.05 were considered statistically significant in all cases. The analysis presented here is exploratory in nature, and thus no adjustments to p-value thresholds were made for potential inflation of Type I error due to multiple comparisons. The inter- and intra-user reliability were assessed using a two-way random intra-class correlation (ICC) model and the coefficient of variation.

RESULTS

Data Summary

Of the originally identified 44 patients, 14 patient data sets were excluded on the bases of semilunar valve regurgitation (>1 L/min by phase contrast measurement; n=4), mixed

ventricular morphology (n=6); severe image artifacts (n=3) or an incomplete data set (n=1). Hence, the final study group consisted of 30 patient data sets (22 males, 8 females). The average age for these patients was 12.7 ± 4.8 years and average body surface area was 1.30 ± 0.38 m^2. In 13 cases, the single ventricle had left ventricular morphology, 17 had a right ventricular morphology. Furthermore, 25 patients had an intra-atrial Fontan connection, while 5 had an extracardiac. In general, all patients were ambulatory, free from significant arrhythmias, and were classified in NYHA Class I or II. Given the relatively small numbers in each of these sub-categories, no separate analyses were performed on the bases of ventricular morphology; however, in these patients, there were no differences in ventricular volumes or ejection fraction between single left and single right ventricles (data not shown).

The ventricular volume data for all 30 patients are presented in Table 2. All volumes were normalized by body surface area to correct for patient size differences. Based on the ejection fraction (56.4 ± 8.9%) and cardiac index (defined as the ventricular output indexed to body surface area, 3.2 ± 0.9 liters/minute/$meter^2$), the systolic performance of these patients was generally preserved(4). The time rate of volume changes and associated time to peak filling are also summarized in Table 2.

Figure 2 shows examples of the output from CFD simulations of the TCPC connections with the lowest (2A) and highest (2B) values for the flow-independent power loss index recorded across the patient subset. Figure 2B in particular highlights a case in which the transition from a constricted Fontan pathway to a dilated connection creates a high velocity jet and complex recirculating flow patterns, all of which contribute to high calculated indexed power losses (0.122). In the entire cohort, the iPL ranged from 0.010-0.122 with a median value of 0.035.

Variable Correlates

Table 3 shows the correlations of ventricular function with the natural logarithm of iPL (based on the visual goodness-of-fit of the data). Statistically significant moderate negative correlations were identified between iPL and ventricular volumes (see Figure 3) and the time to peak filling rate. After controlling for end diastolic volume with partial correlation, associations of iPL with end systolic and stroke volumes were no longer observed.

Reproducibility

The inter-observer variability was assessed using a two-way random intra-class correlation model and combining the independent measures of end diastolic and end systolic volumes for the respective comparisons. These results are summarized in Table 4, along with the coefficient of variation for each variable. All results demonstrated good reproducibility, with all coefficients of variation ≤13%. The end diastolic comparisons had the lowest variability, while the stroke volume had the highest variability (compounding effects of individual errors in the individual volume measurements). Furthermore, the intra-class correlation coefficient for both inter- and intra-observer measures was >0.9, indicating excellent reliability in the results.

COMMENT

Numerous studies have focused on single ventricle mechanics and function as a means to better understand and manage Fontan physiology. The general consensus from these works is that single ventricles post-Fontan experience both systolic and diastolic myocardial dysfunction concurrent with altered arterial and venous hemodynamics and potential disruption of electrical conduction(22); in some cases these findings have been related to increased mortality(13). The novelty of this study is the explicit comparison of TCPC power loss to parameters of ventricular function assessed by CMR. While it has been hypothesized that an inefficient TCPC could negatively impact the function and long-term cardiovascular health of the single ventricle, evidence to support such ideas has been lacking. This study therefore represents a novel contribution as the first concurrent characterization and comparison of ventricular function and TCPC power loss in single ventricle patients.

In support of the stated hypothesis, the primary findings from this study are the moderate negative correlations of flow-independent power loss with end diastolic volume and stroke volume, and the positive association of power loss with time to the peak ventricular filling rate. Collectively, these findings provide compelling evidence that sub-optimal TCPC geometry and adverse hemodynamics may negatively impact ventricular filling and preload. With a higher power loss, there is less ventricular preload, translating to a lower stroke volume which may lead to a decreased cardiac index. Importantly, these associations were observed in generally healthy single ventricle patients under baseline resting conditions, when power loss may be relatively low. Since power loss is known to increase significantly with exercise, the strength and relevance of these associations may be greater under more representative conditions of physiologic exertion. Thus, as impaired diastolic performance is a frequent complication in Fontan physiology(4), these data suggest that the surgically created TCPC may be among the contributing factors if its design creates elevated power loss.

In the absence of a pulmonary pumping chamber, the central venous pressure is the driving pressure for the pulmonary circuit in Fontan physiology. The resistance downstream of this head pressure (i.e., between the central veins and the single ventricle) is the sum total of the TCPC, the pulmonary vasculature (both artery and vein), the atrium, and the atrioventricular valve resistances. Theoretically, if the resistance of any of these individual elements is elevated, such as the TCPC, at least one or more of these components must decrease to compensate or the filling of the ventricle is reduced(23). This cascading mechanism of deleterious TCPC effects is consistent with the present data and our previous findings of an inverse relationship between power loss and systemic venous flow rate(20). Conversely, a recent study found that increased end diastolic volume was an independent predictor of decreased late survival in single ventricle patients(13). This finding could represent a separate mode of Fontan failure that is consistent with systolic dysfunction or chronic volume overload than preload and filling restrictions.

In contrast to the present findings, recent efforts at multi-scale modeling of the Fontan connection and single ventricle physiology have reported no effect of TCPC power loss on single ventricle function(24). These studies relied on a limited number of subjects and

focused solely on the acute peri-operative physiology, which is not inclusive of substantial systemic venous remodeling that is known to occur(25). The reported lack of an association in those models may therefore be reflective of those limitations rather than a true representation of chronic Fontan physiology. By comparison, a lumped parameter modeling study relying on data from a larger and older patient group also demonstrated an effect of TCPC power loss on ventricular preload(26), which agrees well with the present findings of ventricular function directly measured using cardiac magnetic resonance imaging.

We therefore believe that these data provide sufficient evidence that continued investigations into TCPC hemodynamics and power losses and their connection with ventricular function and clinical outcome are warranted. Replication of these findings in a larger prospective cohort and relating elevated flow-independent power losses to poorer long-term outcomes are needed to ultimately confirm the study hypothesis. If true, then minimizing power losses at a patient specific level would help optimize ventricular filling and preload and maintain cardiac output over the long term. Investigations into Fontan surgical planning(27, 28) and the novel Fontan Y-Graft procedure(29, 30) are two forward-looking possibilities for achieving these goals.

This work is subject to several limitations. Time-averaged flow conditions and rigid vessel walls were assumed for CFD, which may introduce a small quantitative bias in the results compared to actual physiologic values. This simplification was necessitated by the lack of sufficient data in all cases to add factors like respiration into the models. Fenestration flow, if present, was systematically ignored, but since it has previously been shown to account for less than 10% of systemic flow(20), that assumption is acceptable.

Since patient-specific flow measurements were used to inform these outflow boundary conditions, only relative differences in patient-specific pulmonary vascular resistances between the left and right pulmonary circuits are accounted for in the model. Magnitude differences in pulmonary vascular resistance among patients are not included in this model and thus represent a separate and independent variable from the reported power loss that also influences ventricular filling and preload. Future work will need to evaluate the relative impacts of pulmonary vascular resistance and TCPC power loss on the ventricle.

The effects of aortic to pulmonary collateral flow on ventricular function and its effect on iPL was not investigated in this study. The result of this collateral flow is volume loading the ventricle and therefore represents a co-variate in this study; if anything, taking this factor into account might strengthen the association between iPL and ventricular function and therefore, we feel that our conclusions are valid.

In conclusion, elevated flow-independent TCPC power losses are associated with decreased ventricular volumes, most notably end diastolic and stroke volumes, and increased time to peak ventricular filling. These findings are important given the fact that the single ventricle output is largely mediated by preload(31), which is typically reserve limited(6), as well as the prevalence of impaired diastolic performance among the single ventricle population(4). While it is not suggested that the TCPC is the primary factor or mediator of these problems,

TCPC hemodynamics can be controlled via surgical intervention, thus providing at least one way to actively pursue better long term outcomes.

ACKNOWLEDGEMENTS

This study was supported by NIH Grants R01HL67622 and R01HL098252, and a Pre-Doctoral Fellowship (10PRE3720002) from the American Heart Association. The authors would like acknowledge the contributions of Veronica O'Connor, RN, BSN and Ravi Doddasomayajula, MS as clinical research coordinators at CHOP.

REFERENCES

1. Gersony DR, Gersony WM. Management of the postoperative fontan patient. Progress in Pediatric Cardiology. 2003; 17:73–79.
2. Cavalcanti S, Gnudi G, Mesetti P, Ussia G, Macelletti C. Analysis by mathematical model of haemodynamic data in the failing fontan circulation. Physiological Measurement. 2001; 22:209–222. [PubMed: 11236882]
3. Eicken A, Fratz S, Gutfried C, et al. Hearts late after fontan operation have normal mass, normal volume, and reduced systolic function. Journal of the American College of Cardiology. 2003; 42:1061–1065. [PubMed: 13678931]
4. Anderson PAW, Sleeper LA, Mahony L, et al. Contemporary outcomes after the fontan procedure. Journal of the American College of Cardiology. 2008; 52(2):85–98. [PubMed: 18598886]
5. Cheung Y, Penny D, Redington A. Serial assessment of left ventricular diastolic function after fontan procedure. Heart. 2000; 83:420–424. [PubMed: 10722541]
6. Senzaki H, Masutani S, Ishido H, et al. Cardiac rest and reserve function in patients with fontan circulation. Journal of the American College of Cardiology. 2006; 47:2528–2535. [PubMed: 16781384]
7. de Leval MR, Kilner P, Gewillig M, Bull C. Total cavopulmonary connection: A logical alternative to atriopulmonary connection for complex fontan operations. Journal of Thoracic and Cardiovascular Surgery. 1988; 96(5):682–695. [PubMed: 3184963]
8. Hsia T-Y, Migliavacca F, Pittaccio S, et al. Computational fluid dynamic study of flow optimization in realistic models of the total cavopulmonary connections. Journal of Surgical Research. 2004; 116:305–313. [PubMed: 15013370]
9. Marsden AL, Vignon-Clementel IE, Chan FP, Feinstein JA, Taylor CA. Effects of exercise and respiration on hemodynamic efficiency in cfd simulations of the total cavopulmonary connection. Annals of Biomedical Engineering. 2007; 35(2):250–263. [PubMed: 17171509]
10. Sundareswaran KS, Haggerty CM, de Zelicourt D, et al. Visualization of flow structures in fontan patients using three-dimensional phase contrast magnetic resonance imaging. Journal of Thoracic and Cardiovascular Surgery. 2012; 143:1108–1116. [PubMed: 22088274]
11. Haggerty CM, Kanter KR, Restrepo M, et al. Simulating hemodynamics of the fontan y-graft based on patient-specific in vivo connections. Journal of Thoracic and Cardiovascular Surgery. 2013; 145(3):663–670. [PubMed: 22560957]
12. de Zelicourt D, Ge L, Wang C, Sotiropoulos F, Gilmanov A, Yoganathan AP. Flow simulations in arbitrarily complex cardiovascular anatomies- an unstructured cartesian grid approach. Computers & Fluids. 2009; 38:1749–1762.
13. Kumita, S-i; Cho, K.; Nakajo, H., et al. Assessment of left ventricular diastolic function with electrocardiography-gated myocardial perfusion spect: Comparison with multigated equilibrium radionuclide angiography. Journal of Nuclear Cardiology. 2001; 8(5):568–574. [PubMed: 11593221]
14. Miller TR, Grossman SJ, Schectman KB, Biello DR, Ludbrook PA, Ehsani AA. Left ventricular diastolic filling and its association with age. The American journal of cardiology. 1986; 58(6): 531–535. [PubMed: 3751916]
15. Whitehead KK, Pekkan K, Kitajima HD, Paridon SM, Yoganathan AP, Fogel MA. Nonlinear power loss during exercise in single-ventricle patients after the fontan: Insights from computational fluid dynamics. Circulation. 2007; 116:I-165–I-171. [PubMed: 17846299]

16. de Zelicourt, D. Biomedical Engineering. Georgia Institute of Technology; Atlanta, GA: 2010. Pulsatile fontan hemodynamics and patient-specific surgical planning: A numerical investigation.
17. Gilmanov A, Sotiropoulos F. A hybrid cartesian/immersed boundary method for simulating flows with 3d, geometrically complex, moving bodies. Journal of Computational Physics. 2005; 207:457–492.
18. Frakes D, Smith M, Parks WJ, Sharma S, Fogel M, Yoganathan AP. New techniques for the reconstruction of complex vascular anatomies from mri images. Journal of Cardiovascular Magnetic Resonance. 2005; 7:425–432. [PubMed: 15881525]
19. Sundareswaran KS, Frakes D, Fogel MA, Soerensen DD, Oshinski JN, Yoganathan AP. Optimum fuzzy filters for phase-contrast magnetic resonance imaging segmentation. Journal of Magnetic Resonance Imaging. 2009; 29:155–165. [PubMed: 19097101]
20. Haggerty CM, Restrepo M, Tang E, et al. Fontan hemodynamics from 100 patient-specific cardiac magnetic resonance studies: A computational fluid dynamics analysis. The Journal of Thoracic and Cardiovascular Surgery. 2014; 148(4):1481–1489. [PubMed: 24507891]
21. Dasi LP, Pekkan K, de Zelicourt D, et al. Hemodynamic energy dissipation in the cardiovascular system: Generalized theoretical analysis on disease states. Annals of Biomedical Engineering. 2009; 37(4):661–673. [PubMed: 19224370]
22. Fogel, MA. Ventricular function and blood flow in congenital heart disease. Blackwell Futura; Malden, Mass: 2005.
23. Guyton A, Abernathy B, Langston J, Kaufmann B, Fairchild H. Relative importance of venous and arterial resistances in controlling venous return and cardiac output. American Journal of Physiology. 1959; 196(5):1008–1014. [PubMed: 13649920]
24. Baretta A, Corsini C, Yang W, et al. Virtual surgeries in patients with congenital heart disease: A multi-scale modelling test case. Philosophical Transactions of the Royal Society A. 2011; 369:4316–4330.
25. Kelly J, Mack G, Fahey J. Diminished venous vascular capacitance in patients with univentricular hearts after the fontan operation. American Journal of Cardiology. 1995; 76(3):158–163. [PubMed: 7611151]
26. Sundareswaran KS, Pekkan K, Dasi LP, et al. The total cavopulmonary connection resistance: A significant impact on single ventricle hemodynamics at rest and exercise. American Journal of Physiology Heart and Circulatory Physiology. 2008; 295:H2427–H2435. [PubMed: 18931028]
27. Sundareswaran KS, de Zelicourt D, Sharma S, et al. Correction of pulmonary arteriovenous malformation using image-based surgical planning. Journal of the American College of Cardiology: Cardiovascular Imaging. 2009; 2(8):1024–1030. [PubMed: 19679291]
28. Haggerty CM, de Zelicourt D, Restrepo M, et al. Comparing pre- and post-operative fontan hemodynamic simulations: Implications for the reliability of surgical planning. Annals of Biomedical Engineering. 2012; 40(12):2639–2651. [PubMed: 22777126]
29. Kanter KR, Haggerty CM, Restrepo M, et al. Preliminary clinical experience with a bifurcated y-graft fontan procedure- a feasibility study. Journal of Thoracic and Cardiovascular Surgery. 2012; 144:383–389. [PubMed: 22698555]
30. Marsden AL, Bernstein AJ, Reddy VM, et al. Evaluation of a novel y-shaped extracardiac fontan baffle using computational fluid dynamics. Journal of Thoracic and Cardiovascular Surgery. 2009; 137:394–403. [PubMed: 19185159]
31. Gewillig M, Brown SC, Eyskens B, et al. The fontan circulation: Who controls cardiac output? Interactive CardioVascular and Thoracic Surgery. 2010; 10(3):428–433. [PubMed: 19995891]

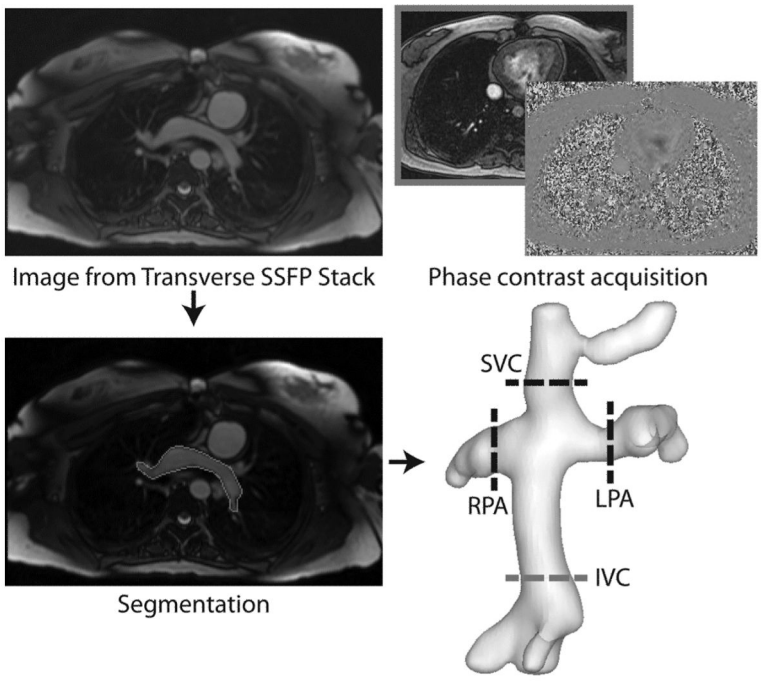

Figure 1.

Imaging inputs required for TCPC computational fluid dynamics simulations: transverse stack of MR images for anatomic reconstruction and through-plane phase contrast MR images to obtain patient-specific flow boundary conditions.

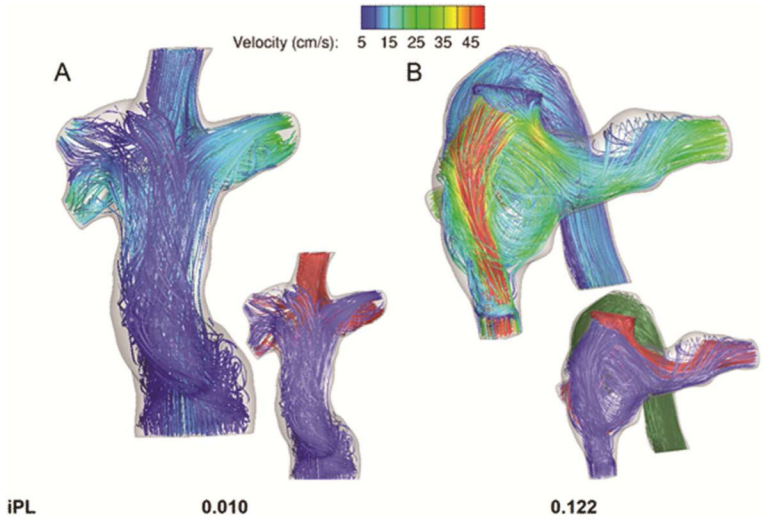

Figure 2.

Representative output for computational fluid dynamics simulations showing time averaged velocity streamlines and iPL for the A) lowest and B) highest power loss patients from among the patients analyzed. In the larger figures, the streamlines are color-coded by local velocity magnitude, while the streamlines in the inset images are color-coded by vessel of origin: red- superior vena cava; blue- inferior vena cava; green- azygos vein.

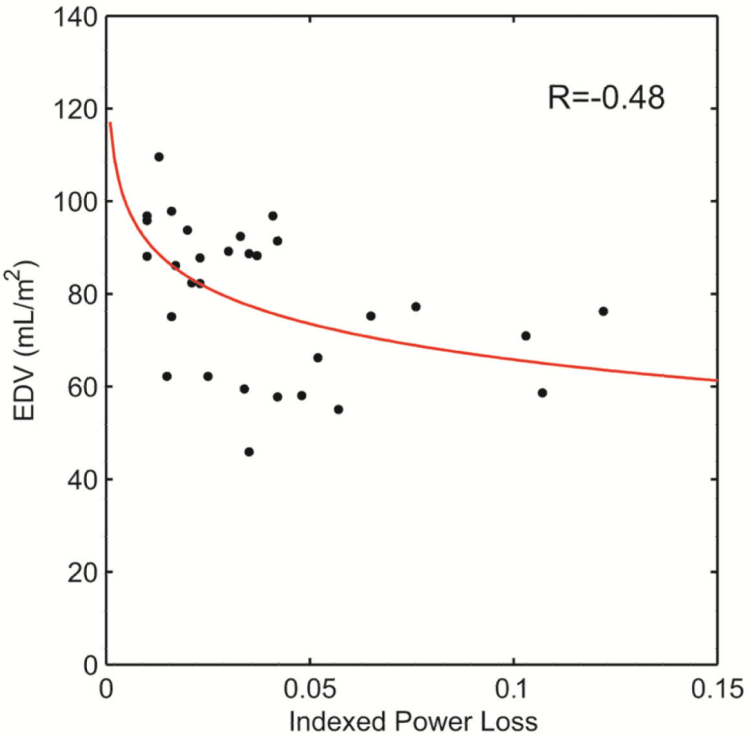

Figure 3.
Statistically significant logarithmic correlations observed between indexed power loss and end diastolic volume (EDV).

Table 1

Cardiac magnetic resonance imaging detail (mean ± st. dev.) for ventricular function, TCPC anatomy and velocity acquisitions

	Ventricular short axis cine stack	Transverse Thoracic stack	Through-plane phase contrast
Slices	7.9 ± 1.0	45.6 ± 6.6	1
Slice Thickness (mm)	8.3 ± 1.3	4.2 ± 0.7	5.6 ± 0.7
Number of Phases per Cardiac Cycle	25.6 ± 4.4	1	25.8 ± 4.2
Phase dt (ms)	34 ± 5	NA	33 ± 6
In-Plane Spatial Resolution (mm)	1.35 ± 0.37	1.16 ± 0.22	1.16 ± 0.25

Table 2

Summary of Ventricular Function Measures

	End Diastolic Volume (mL/m^2)	End Systolic Volume (mL/m^2)	Stroke Volume (mL/m^2)	Ejection Fraction (%)	Heart Rate (bpm)	CI-VF [$L/min/m^2$]	CI-PC [$L/min/m^2$]	Peak Ejection Rate (s^{-1})	Peak Filling Rate (s^{-1})	Peak filling time ratio
Mean ± Stand. Dev.	78.9 ± 16.0	34.7 ± 11.7	44.2 ± 9.8	56.4 ± 8.9	73.6 ± 17.0	3.2 ± 0.9	3.5 ± 0.7	3.16 ± 1.04	2.68 ± 0.88	0.18 ± 0.05

CI-VF Cardiac Index derived from ventricle segmentation; CI-PC Cardiac Index derived from phase contrast measurement in the ascending aorta; Rates normalized to end diastolic volume

Table 3

Correlations of Natural Logarithm of iPL with ventricular function

	Correlation with Correlation coefficient (R)	***In (iPL) p-value***
End Systolic Volume [mL/BSA]	−0.37*	0.047
End Diastolic Volume [mL/BSA]	−0.48*	0.006
Stroke Volume [mL/BSA]	−0.37*	0.047
Ejection Fraction [%]	0.10	0.611
Peak Ejection Rate [s^{-1}]	0.162	0.393
Peak Filling Rate [s^{-1}]	0.107	0.572
CI-VF *[L/min/m^2]*	−0.038	0.841
CI-PC *[L/min/m^2]*	−0.078	0.681
Time ratio to peak filling	0.67*	<0.001
Heart Rate (bpm)	0.29	0.121

In(iPL) – natural logarithm of iPL; segmentation; CI-PC Cardiac Index derive ascending aorta; Rates norm CI-VF Cardiac Index derived from ventricle ed from phase contrast measurement in the alized to end diastolic volume

* $p<0.05$;

Table 4

Results of the user variability analyses

	Coefficient of Variation (%)					
	End Diastolic Volume	**End Systolic Volume**	**Stroke Volume**	**Peak Ejection Rate**	**Peak Filling Rate**	**Intra-Class Correlation coefficient**
Inter-observer (n=8)	8	10	13	N/A	N/A	0.935
Intra-observer (n=5)	3	5	7	10	11	0.993